

# Robust DOA Estimation of Complex Correlated Signals in Non-Gaussian CES Distributed Models

Habti Abeida<sup>1</sup>

**Abstract:** The sample covariance matrix (SCM) is commonly used in direction-of-arrival (DOA) estimation methods when the noise or observations are circular complex Gaussian (C CG) distributed. However, with a very heavy-tailed non-Gaussian noise model, the SCM-based DOA estimation methods fail to provide an accurate estimate of DOA. This paper presents a numerical analysis of the resolving capability of subspace-based circular (C) and non-circular (NC) multiple signal classification (MUSIC) DOA estimation methods of arbitrarily narrowband correlated signal sources corrupted by circular complex elliptical symmetric (C CES) distributed noise. It evaluates the robustness of these methods for correlated C and NC sources by employing the robust complex M –estimators instead of SCM. It study also the effects of correlation on robust MUSIC-based DOA estimation algorithms accuracy as a function of the magnitude and phase of the correlation coefficients. Simulations results show that the NC MUSIC algorithm which requires fewer sensor elements yields robust estimates of DOA for correlated sources than the C MUSIC algorithm using the M –estimators.

**Keywords:** DOA estimation, Correlated signal sources, Heavy-tailed non-Gaussian noise and observations, Complex elliptical symmetric distributions, Robust M –estimators.

## 1 Introduction

The most commonly subspace-based methods for estimating the DOA of closely-spaced C and NC sources are respectively the C MUSIC [1] and NC MUSIC [2] methods due to their simplicity and high-precision capability [3, 4]. It is well-known that these methods can resolve two uncorrelated sources. However, these methods encounter significant difficulties in accurately estimating the DOAs when the signals are highly correlated [5, 6], which can occur in the case of multipath propagation or smart jammer scenarios. Up till now, several subspace-based approaches (spatial smoothing, spatial filtering) have been developed to decorrelate strongly correlated C signals (e.g., [7 – 11]).

---

<sup>1</sup>Taif University, College of Engineering, Dept. of Electrical Engineering, Al-Haweiah, 21974, Saudi Arabia  
E-mail: h.abeida@tu.edu.sa

The decorrelation subspace-based approaches are inspired by the first works proposed in [12 – 15].

In array signal processing applications, C and NC MUSIC-based methods and the maximum likelihood (ML) method require an estimate of the covariance matrix (CM). The most commonly used estimator of CM under a multivariate Gaussian assumption is the SCM which is an ML estimate. However, the use of SCM in non-Gaussian outliers or impulsive noise scenarios can be modeled by C CES distributions [17] leads to degraded estimation performance of the DOA. Moreover, a robust alternative estimate to the SCM is the M – estimators introduced in [16] for real-valued data, and then extended for C and NC CES distributed data in [17] and [18], respectively. These robust M – estimators have been widely used and studied in various statistical signal processing applications [17, 23 – 26].

This paper studies the accuracy of the C and NC MUSIC-based DOA estimation methods as a function of correlation magnitude and phase between signal sources. It quantifies then the robustness of these methods for estimating DOAs of correlated closely-spaced sources in the non-Gaussian C CES noise environment, by employing the M – estimators instead of SCM.

The paper is structured as follows. A brief reminder of NC CES distributions is presented in Section 2. Section 3 presents robust C and NC CES distributed models and M – estimators. Section 4 presents the C and NC signal models and briefly reminds the C and NC MUSIC algorithms designed for DOA estimation of correlated signal sources. Simulation results are presented in Section 5 to assess the dependence of MUSIC-based DOA estimation methods on the correlation magnitude and phase of sources and also evaluate the robustness of the M – estimators. Finally, the conclusion is presented in Section 6.

## 2 NC CES Distributions

A generalization of C CES distributions [17, 21] called NC CES distributions has been introduced in [20] so that the NC CG distribution [22] belongs to this family of distributions. A random variable (r.v.)  $\mathbf{z}_t \in \mathbb{C}^M$  follows an NC CES distribution  $\mathbf{z}_t \sim EC_M(\boldsymbol{\mu}_t, \boldsymbol{\Sigma}, \boldsymbol{\Omega}, g)$  if its probability density function (p.d.f.) has the form

$$f(\mathbf{z}_t) = c_{M,g} |\tilde{\boldsymbol{\Gamma}}|^{-1/2} g(\tilde{\eta}(\mathbf{z}_t)), \quad (1)$$

where  $\tilde{\eta}(\mathbf{z}_t)$  is the quadratic form,  $\tilde{\eta}(\mathbf{z}_t) \stackrel{\text{def}}{=} \frac{1}{2} (\tilde{\mathbf{z}}_t - \tilde{\boldsymbol{\mu}}_t)^H \tilde{\boldsymbol{\Gamma}}^{-1} (\tilde{\mathbf{z}}_t - \tilde{\boldsymbol{\mu}}_t)$  and where

$\tilde{\mathbf{z}}_t \stackrel{\text{def}}{=} (\mathbf{z}_t^H \ \mathbf{z}_t^T)^H$ ,  $\tilde{\boldsymbol{\mu}}_t \stackrel{\text{def}}{=} (\boldsymbol{\mu}_t^H \ \boldsymbol{\mu}_t^T)^H$  and  $\tilde{\boldsymbol{\Gamma}} \stackrel{\text{def}}{=} \begin{pmatrix} \boldsymbol{\Sigma} & \boldsymbol{\Omega} \\ \boldsymbol{\Omega}^* & \boldsymbol{\Sigma}^* \end{pmatrix}$ ,  $\boldsymbol{\Sigma} \in \mathbb{C}^{M \times M}$  and  $\boldsymbol{\Omega} \in \mathbb{C}^{M \times M}$  are

respectively Hermitian positive definite scatter matrix with  $\text{rank}(\boldsymbol{\Sigma}) = M$  and complex symmetric pseudo-scatter matrix. The coefficient  $c_{M,g} \stackrel{\text{def}}{=} 2(s_M \delta_{M,g})^{-1}$  is a normalizing constant ensuring that (1) integrates to one and where  $\delta_{M,g} = \int_0^\infty u^{M-1} g(u) du < \infty$  and  $s_M \stackrel{\text{def}}{=} 2\pi^M / \Gamma(M)$  is the surface area of the unit complex  $m$ -sphere  $\mathbb{CS}^M = \{\mathbf{z}_t \in \mathbb{C}^M : \|\mathbf{z}_t\| = 1\}$ . The non-negative density generator function  $g(\cdot)$  is assumed here to satisfy  $\delta_{M+1,g} / \delta_{M,g} = M$  [17] to ensure that  $\boldsymbol{\Sigma} = \mathbf{R}_z \stackrel{\text{def}}{=} \mathbb{E}(\mathbf{z}_t \mathbf{z}_t^H)$ ,  $\boldsymbol{\Omega} = \mathbf{R}'_z \stackrel{\text{def}}{=} \mathbb{E}(\mathbf{z}_t \mathbf{z}_t^T)$  and  $\tilde{\mathbf{I}} = \mathbf{R}_{\tilde{z}} \stackrel{\text{def}}{=} \mathbb{E}(\tilde{\mathbf{z}}_t \tilde{\mathbf{z}}_t^H)$ . It follows from [27, Corollary 4.6.12(b)], that the matrices  $\boldsymbol{\Sigma}$  and  $\boldsymbol{\Omega}$  can be factorized as  $\boldsymbol{\Sigma} = \mathbf{A}\mathbf{A}^H$  and  $\boldsymbol{\Omega} = \mathbf{A}\mathbf{A}\mathbf{A}^T$ , where  $\mathbf{A} \in \mathbb{C}^{M \times M}$  is a non-singular matrix and  $\mathbf{A} = \text{Diag}(\kappa_1, \dots, \kappa_M)$  is a diagonal matrix with nonnegative real elements. Let  $\mathbf{v}_t \in \mathbb{C}^M$  be an r.v. obtained using a simple transformation of r.v.  $\mathbf{u}_t \in \mathbb{C}^M$  uniformly distributed on  $\mathbb{CS}^M$  (i.e.,  $\mathbf{u}_t \sim U(\mathbb{CS}^M)$ ) as follows [19]:

$$\mathbf{v}_t = \mathbf{A}_1 \mathbf{u}_t + \mathbf{A}_2 \mathbf{u}_t^*, \quad (2)$$

with  $\mathbf{A}_1 = \frac{\mathbf{A}_+ + \mathbf{A}}{2}$  and  $\mathbf{A}_2 = \frac{\mathbf{A}_+ - \mathbf{A}}{2}$ , where  $\mathbf{A}_+ = \sqrt{\mathbf{I} + \mathbf{A}}$  and  $\mathbf{A}_- = \sqrt{\mathbf{I} - \mathbf{A}}$ .

Clearly,  $\mathbb{E}(\mathbf{v}_t \mathbf{v}_t^H) = \mathbb{E}(\mathbf{u}_t \mathbf{u}_t^H) = \frac{1}{M} \mathbf{I}$  and  $\mathbb{E}(\mathbf{v}_t \mathbf{v}_t^T) = \frac{1}{M} \mathbf{A}$ . Therefore, an r.v.  $\mathbf{z}_t \sim \text{EC}_M(\boldsymbol{\mu}_t, \boldsymbol{\Sigma}, \boldsymbol{\Omega}, g)$  with  $\text{rank}(\boldsymbol{\Sigma}) = M$  if its stochastic representation (SR) has the form

$$\mathbf{z}_t =_d \boldsymbol{\mu}_t + \mathcal{R}_t \mathbf{A} \mathbf{v}_t, \quad (3)$$

with  $\mathcal{R}_t$  is the modular variate defined as  $\mathcal{R}_t \stackrel{\text{def}}{=} \sqrt{Q_t}$  which is independent of the complex r.v.  $\mathbf{v}_t$ . The p.d.f. of  $Q_t$  is given by

$$f(Q_t) = \delta_{M,g}^{-1} Q_t^{M-1} g(Q_t).$$

The density generator function of an NC CG distribution is  $g(t) = e^{-t}$ . In the particular case  $\boldsymbol{\Omega} = 0$  the NC CG distribution reduces to the C CG distribution. *Zero-mean complex Student's  $t$ -distribution* [17]: An r.v.  $\mathbf{z}_t$  follows a complex Student's  $t$ -distribution (denoted as  $\mathbb{C}t_{M,\nu}(\boldsymbol{\theta}, \boldsymbol{\Sigma})$ ) with  $\nu$  ( $0 < \nu < \infty$ ) degrees of freedom if the corresponding SR admits  $Q_t =_d M F_{2M,\nu}$ , where  $F_{2M,\nu}$  denotes the  $F$ -distribution with  $(2M, \nu)$  degrees of freedom. The complex  $t$ -distribution has tails heavier than CG ( $\nu \rightarrow \infty$ ). The case  $\nu = 1$  leads to the complex Cauchy

distribution, and the case  $\nu = 1/2$  yields the multivariate Laplace distribution which is heavy-tailed distribution. Thus, the complex Student's  $t$ -distribution was chosen here in preference to other possible robust distributions to evaluate the robustness of C and NC MUSIC-based DOA estimation methods for C and NC correlated signal sources.

### 3 Robust C and NC CES Distributed Models and M-Estimators

Unlike model (6) which assumes that the noise is C CES, this section presents an alternative model where the observations  $z_t$  in (6) are assumed to be independent with zero-mean either C or NC CES with respective scattering matrix  $\mathbf{R}_z$  or  $\mathbf{R}_{\tilde{z}}$ . This model is also used to quantify the effects of correlation on C and NC MUSIC-based DOA estimation methods using the M – estimators. Usually, the C and NC noise subspaces from which the C and NC MUSIC algorithms are built are estimated, respectively, using the SCM  $\mathbf{R}_{z,T} \stackrel{\text{def}}{=} \frac{1}{T} \sum_{t=1}^T z_t z_t^H$  and the extended SCM  $\mathbf{R}_{\tilde{z},T} \stackrel{\text{def}}{=} \frac{1}{T} \sum_{t=1}^T \tilde{z}_t \tilde{z}_t^H$ . They are ML estimators of  $\Sigma$  and  $\tilde{\Gamma}$  for C CG and NC CG distributed data, respectively. However, the performance of SCM-based MUSIC methods significantly degrades in heavy-tailed CES distributed data. An alternative robust ML M – estimator to the SCM and extended SCM are defined respectively as the solution of the M – estimating equations [17, 18]

$$\mathbf{R}_{z,T} = \frac{1}{T} \sum_{t=1}^T \phi(z_t^H \mathbf{R}_{z,T}^{-1} z_t) z_t z_t^H \quad (4)$$

$$\mathbf{R}_{\tilde{z},T} = \frac{1}{T} \sum_{t=1}^T \phi\left(\frac{1}{2} \tilde{z}_t^H \mathbf{R}_{\tilde{z},T}^{-1} \tilde{z}_t\right) \tilde{z}_t \tilde{z}_t^H, \quad (5)$$

where  $\phi(t) \stackrel{\text{def}}{=} -\frac{1}{g(t)} \frac{d g(t)}{d t}$ .

In the particular case of CG distribution for which  $g(t) = e^{-t}$  yields  $\phi(t) = 1$ , (4) and (5) reduce respectively to SCM and extended SCM. The unique solution of (4) and (5) can be obtained by an iterative fixed-point algorithm. When  $g(\cdot)$  is unknown, M – estimators can be used to provide reliable estimates of  $\mathbf{R}_z$  and  $\mathbf{R}_{\tilde{z}}$  which are also solutions of the implicit (4) and (5), obtain  $\mathbf{R}_z$  ed by replacing  $\phi(\cdot)$  by any non-negative real-valued weight function  $u(\cdot)$  follows Maronna's conditions [16] and is not tied to any particular CES distribution.

In [18], both the existence and uniqueness of solutions of (5) were proved in [18] extending those proved in [17] for the C CES data. For example, Tyler's and

Huber's estimators are members of the class of  $M$  – estimators (see e.g., [17, sec.V.C]). Tyler's  $M$  – estimator is obtained from (5) by taking  $u(t) = M/t$  while the weight function for Huber's  $M$  – estimators is given in [17, Example 1]. Note also that the weight function  $\phi(\cdot)$  for Student's ML-estimator (denoted as MLT ( $\nu$ )) in (4) and (5) is given by  $\phi(t) = \frac{2M + \nu}{\nu + 2t}$ . Finally, the normalized sign SCM (SSCM) estimator proposed in [28] is extended for NC CES observations and has the form  $\mathbf{R}_{z,T} \stackrel{\text{def}}{=} \frac{1}{T} \sum_{t=1}^T S(\tilde{z}_t) S^H(\tilde{z}_t)$  with  $S(z_t) \stackrel{\text{def}}{=} z_t / \|z_t\|$  if  $z_t \neq 0$  and  $S(0) \stackrel{\text{def}}{=} 0$ , which is not an  $M$  – estimate of  $\mathbf{R}_z$ , is considered in this study.

## 4 Signal Model for DOA Estimation

This section presents the CES signal model and briefly summarizes the C and NC MUSIC methods (e.g., [3]) for estimating DOAs of arbitrary distributed correlated sources in an impulsive noise environment with heavy-tailed distributions.

### 4.1 Signal model

Assume that two narrowband uncorrelated or correlated signal sources impinge on an array of  $M$  sensor elements. The output of the sensor array at the instant  $t$ , denoted as  $\mathbf{z}_t \in \mathbb{C}^M$ , can be written as [3, 26]

$$\mathbf{z}_t = \mathbf{A}(\boldsymbol{\theta}) \mathbf{s}_t + \mathbf{n}_t, \quad t = 1, \dots, T, \quad (6)$$

where  $\mathbf{z}_t$  are assumed to be independent and identically distributed r.v.'s and  $\mathbf{A}(\boldsymbol{\theta}) = [\mathbf{a}(\theta_1), \mathbf{a}(\theta_2)]$ ,  $\mathbf{a}_k \stackrel{\text{def}}{=} \mathbf{a}(\theta_k)$  is the steering vector corresponding to  $\theta_k \in \mathbb{R}$ . The vectors  $\mathbf{s}_t = (s_{t,1}, s_{t,2}) \in \mathbb{C}^2$  and  $\mathbf{n}_t \in \mathbb{C}^M$  represent respectively the transmitted signal sources and additive measurement noise, which are assumed to have zero-mean and are independent. The noise  $\mathbf{n}_t =_d \sigma_n \sqrt{\mathcal{Q}} \mathbf{u}_t$  is assumed to be C CES distributed constrained such that  $\mathbb{E}(\mathcal{Q}) = M$  to ensure that  $\mathbb{E}(\mathbf{n}_t \mathbf{n}_t^H) = \sigma_n^2 \mathbf{I}$ , whereas the signal sources  $\mathbf{s}_t$  are C or NC arbitrary distributed, with first covariance  $\mathbf{C}_s = \mathbb{E}(\mathbf{s}_t \mathbf{s}_t^H)$  and second covariance  $\mathbf{P}_s = \mathbb{E}(\mathbf{x}_t \mathbf{x}_t^T)$ . Therefore, CMs of the r.v.  $\mathbf{z}_t$  are given by:

$$\mathbf{R}_z = \mathbf{A} \mathbf{C}_s \mathbf{A}^H + \sigma_n^2 \mathbf{I} \quad \text{and} \quad \mathbf{R}'_z = \mathbf{A} \mathbf{P}_s \mathbf{A}^T, \quad (7)$$

where

$$\mathbf{C}_s = \sigma_s^2 \begin{pmatrix} 1 & \rho \\ \rho^* & 1 \end{pmatrix} \quad \text{with} \quad \rho \stackrel{\text{def}}{=} \mathbb{E}(s_{t,1} s_{t,2}^*) = |\rho| e^{i\angle \rho} \in \mathbb{C}, \quad |\rho| < 1. \quad (8)$$

For the particular case of strictly rectilinear signals  $s_{t,1}$  and  $s_{t,2}$ , we have:

$$s_{t,k} = x_{t,k} e^{i\phi_k}, \quad x_{t,k} \in \mathbb{R} \quad \text{with} \quad \Delta\phi \stackrel{\text{def}}{=} \phi_1 - \phi_2 \in [0, +\pi], \quad (9)$$

where the phases  $\phi_k$  are assumed fixed during the array observation. Consequently, this leads to the CMs:

$$\mathbf{R}_z = \mathbf{A}(\boldsymbol{\theta})\mathbf{C}_s\mathbf{A}(\boldsymbol{\theta})^H + \sigma_n^2\mathbf{I} \quad \text{and} \quad \mathbf{R}'_z = \mathbf{A}(\boldsymbol{\theta})\mathbf{P}_s\mathbf{A}(\boldsymbol{\theta})^T.$$

To exploit the prior knowledge of rectilinear sources, the augmented CM of the r.v.  $\tilde{\mathbf{z}}_t = (\mathbf{z}_t^T \mathbf{z}_t^H)^T$  defined in Section 2, can be written as [3]:

$$\mathbf{R}_{\tilde{\mathbf{z}}} = \begin{pmatrix} \mathbf{R}_z & \mathbf{R}'_z \\ \mathbf{R}'_z^* & \mathbf{R}_z^* \end{pmatrix} = \begin{pmatrix} \mathbf{A}\mathbf{A}_\phi \\ \mathbf{A}^*\mathbf{A}'_\phi \end{pmatrix} \mathbf{C}_x \begin{pmatrix} \mathbf{A}\mathbf{A}_\phi \\ \mathbf{A}^*\mathbf{A}'_\phi \end{pmatrix}^H + \sigma_n^2\mathbf{I} \quad (10)$$

with  $\mathbf{A}_\phi \stackrel{\text{def}}{=} \text{Diag}(\phi_1, \phi_2)$ , where if

$$\mathbf{C}_x \stackrel{\text{def}}{=} \mathbb{E}(\mathbf{x}_t \mathbf{x}_t^T) = \sigma_x^2 \begin{pmatrix} 1 & \rho' \\ \rho' & 1 \end{pmatrix}, \quad \rho' \in (-1, +1), \quad (11)$$

$\mathbf{C}_s$  in (8) has the following form:

$$\mathbf{C}_s = \sigma_x^2 \begin{pmatrix} 1 & \rho' e^{i\Delta\phi} \\ \rho' e^{-i\Delta\phi} & 1 \end{pmatrix} \quad (12)$$

It follows, therefore, from (8) and (12) that the non-circularity phase separation  $\Delta\phi$  associated with the sign of real-valued factor  $\rho'$  corresponds to the correlation phase  $\angle\rho$  of signal sources.

## 4.2 C and NC MUSIC-based DOA estimation algorithms

The NC MUSIC algorithm [2, 3] estimates the two DOAs as the location of the two smallest minima of the following spatial spectrum defined by:

$$f_T(\theta) = (\mathbf{a}^H(\theta)\mathbf{\Pi}_{1,T}\mathbf{a}(\theta))^2 - |\mathbf{a}^T(\theta)\mathbf{\Pi}_{2,T}^*\mathbf{a}(\theta)|^2,$$

where  $\mathbf{\Pi}_{1,T}$  is a Hermitian matrix and  $\mathbf{\Pi}_{2,T}$  is a complex symmetric matrix obtained both from the partitioned null-space projection matrix,

$$\tilde{\mathbf{\Pi}}_T = \begin{pmatrix} \mathbf{\Pi}_{1,T} & \mathbf{\Pi}_{2,T} \\ \mathbf{\Pi}_{2,T}^* & \mathbf{\Pi}_{1,T} \end{pmatrix},$$

associated with the noise subspace of the estimated matrix  $\mathbf{R}_{\tilde{\mathbf{z}},T}$ .

Similarly, the C MUSIC algorithm [1] estimates the two DOAs as the location of the two smallest minima of the following spatial spectrum defined by:  $g_T(\theta) = \mathbf{a}^H(\theta)\mathbf{\Pi}_T\mathbf{a}(\theta)$ , where  $\mathbf{\Pi}_T$  is the projector matrix associated with the noise subspace of  $\mathbf{R}_{z,T}$ .

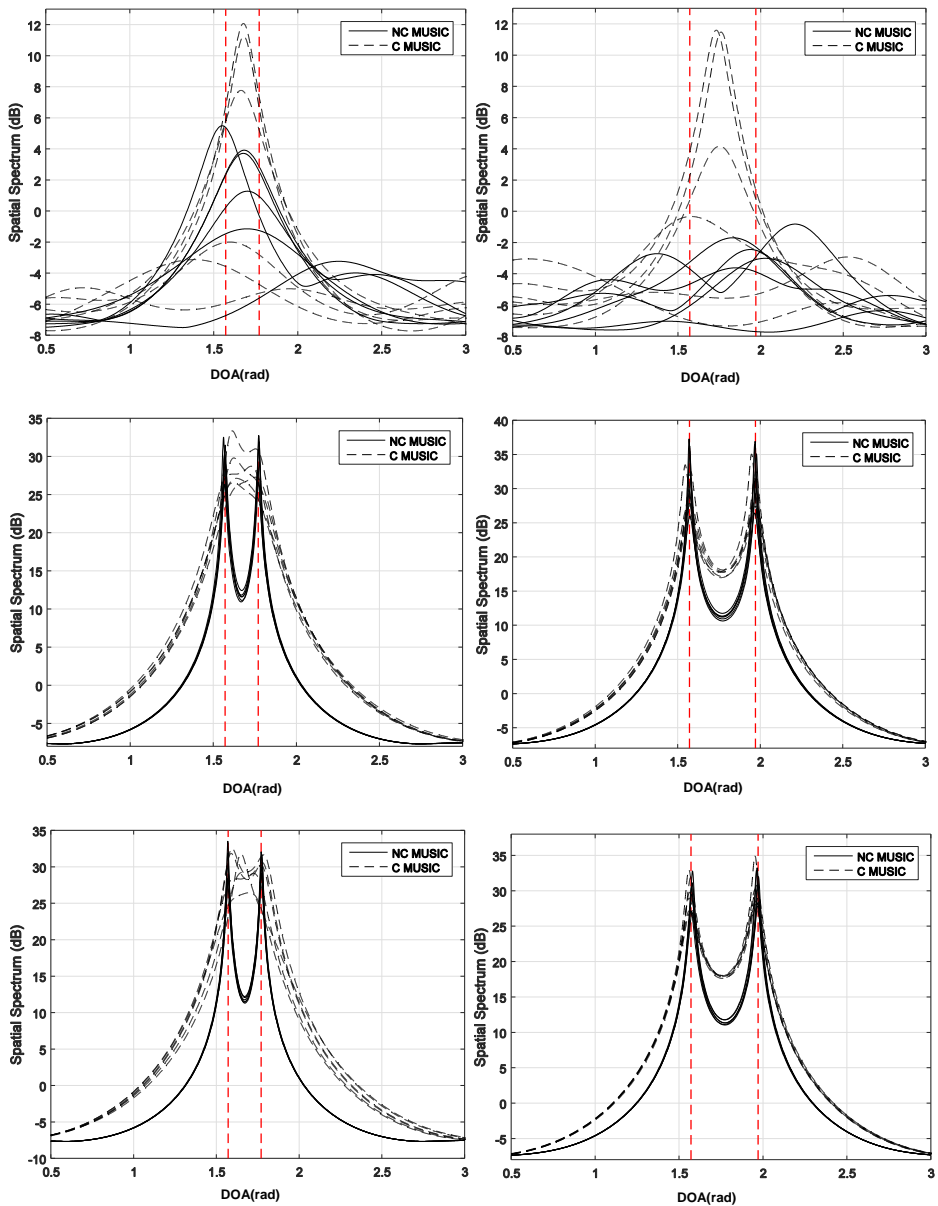
## 5 Simulation Results and Discussion

This section presents several numerical simulations to illustrate the dependence of the performance of C and NC MUSIC-based DOA estimation methods on the non-Gaussian heavy-tailed noise or data and the correlation phase and magnitude of correlated signal sources.

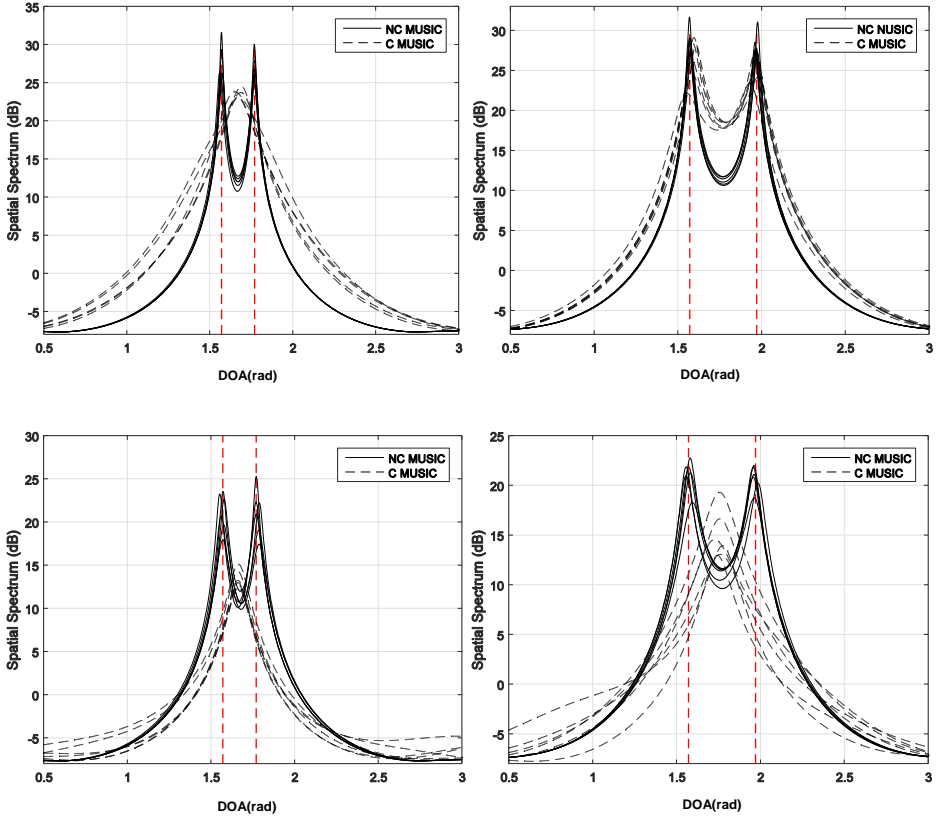
Assume that there are two correlated narrowband rectilinear signal sources with the same power  $\sigma_x^2$  impinging on a uniform linear array with  $M = 6$  (except in Fig. 4) omnidirectional sensors spaced half-wavelength for which  $\mathbf{a}_k = (1, e^{j\theta_k}, \dots, e^{j(M-1)\theta_k})^T$  with  $\theta_k = \sin(\pi\alpha_k)$ , where  $\alpha_k$  is DOA relative to the normal of array broadside. The two sources are generated as in model (6) which consists of two multi-paths issued from two independent BPSK-modulated sources  $e_{t,1}$  and  $e_{t,2}$  such as  $x_{t,1} = e_{t,1}$  and  $x_{t,2} = \rho' e_{t,1} + \sqrt{1-\rho'^2} e_{t,2}$  with  $\rho' \in (-1, +1)$ . Thus, the signal sources  $s_{t,1}$  and  $s_{t,2}$  are correlated with correlation  $\rho = \rho' e^{i\Delta\phi}$ , where  $\Delta\phi = \phi_2 - \phi_1$ . The number of snapshots is set to 500.

Figure 1 shows the C and NC MUSIC spatial spectrums based on the following estimators presented in Section 3: SCM, ML-estimator based on Student's  $t$ -distribution MLT(1) with  $\phi(t) = \frac{2M + v}{v + 2t}$ , Tyler's M-estimator, Huber's M-estimator with  $q = 0.9$  and SSCM. The two sources are assumed highly correlated with  $|\rho| = \rho' = 0.95$ , and the non-Gaussian heavy-tailed noise  $\mathbf{n}_t$ , is assumed to follow  $\mathcal{C}t_{M,v}$  with  $v = 1$  (i.e., the complex Cauchy distribution). Since the complex Cauchy distribution has infinite variance, then  $\sigma_n^2$  refers here its dispersion parameter, and the generalized SNR is defined as  $10\log_{10}(\sigma_s^2 / \sigma_n^2) = 20\text{dB}$ .

It can be observed from Fig. 1 that the C and NC MUSIC algorithms based on classical SCM estimator fail to resolve two far or close sources in non-Gaussian heavy-tailed noise. In addition, the SSCM-based C MUSIC algorithm does not separate the two sources, unlike the SSCM-based NC MUSIC algorithm which performs well in this case. On the one hand, the NC MUSIC algorithm provides reliable estimates of the DOA's for both far or close correlated sources using the robust estimators MLT(1), Tyler's and Huber's estimators, while the performance of the C MUSIC algorithm is enhanced with the use of these robust estimators which make it produces reliable estimates of DOA's of two correlated sources for large DOA separation  $\Delta\theta$ .



**Fig. 1a** – C and NC MUSIC spatial spectrum of two correlated signal sources with  $|\rho| = \rho' = 0.95$  and  $\angle \rho = \Delta\phi = \pi/2$  built using SCM (and extended SCM) (first row), MLT(1) (second row), Tyler's  $M$ -estimator (third row), for five simulated data. The curves are plotted for two values of DOA separation:  $\Delta\theta = |\theta_2 - \theta_1| = 0.2$  rad (first column) and  $\Delta\theta = 0.4$  rad (second column).



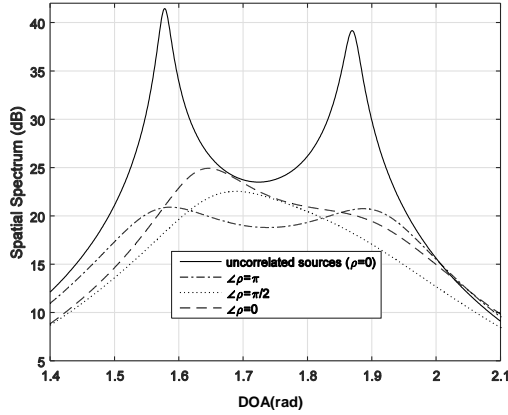
**Fig. 1b** – *C* and NC MUSIC spatial spectrum of two correlated signal sources with  $|\rho| = \rho' = 0.95$  and  $\angle \rho = \Delta\phi = \pi/2$  built using Huber's  $M$ -estimator with  $q = 0.9$  (first row) and SSCM (second row) for five simulated data.

The curves are plotted for two values of DOA separation:  $\Delta\theta = |\theta_2 - \theta_1| = 0.2$  rad (first column) and  $\Delta\theta = 0.4$  rad (second column).

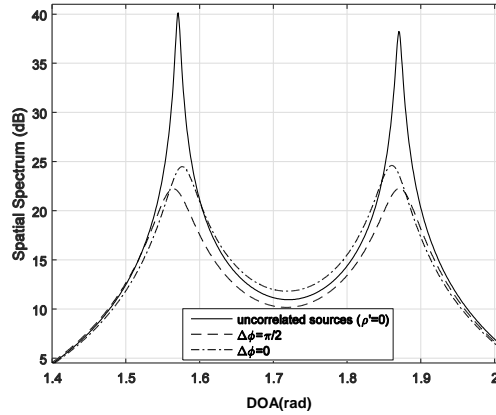
Figs. 2 – 4 show the influence of the magnitude and phase correlation (i.e.,  $|\rho| = \rho'$  and  $\angle \rho = \Delta\phi$ ) on C and NC MUSIC algorithms. The noise vector  $\mathbf{n}_t$  is generated according to the  $\mathbb{C}t_{M,\nu}$  with  $\nu = 3$ . The estimated projector  $\mathbf{\Pi}_T$  [resp.  $\tilde{\mathbf{\Pi}}_T$ ] are obtained using MLT(3) given by (4) [resp. (5)] with  $\phi(t) = \frac{2M + \nu}{\nu + 2t}$ .

In Fig. 2, the C and NC MUSIC pseudo-spectrums for the case of uncorrelated sources ( $|\rho| = \rho' = 0$ ) are also included.

It can be observed from this figure that the C MUSIC algorithm is unable to resolve the two closely highly correlated sources with  $\angle\rho = 0$  and  $\angle\rho = \pi/2$  which is not the case with the NC MUSIC algorithm. While the C MUSIC algorithm, as well as the NC MUSIC algorithm, are capable of resolving two uncorrelated sources, it is important to note that the C MUSIC pseudo-spectrum shows two weak peaks for  $\angle\rho = \pi$  implying that the coherent sources can be resolved even though  $|\rho|=1$  where  $\mathbf{C}_s$  is singular.



C MUSIC  
(a)



NC MUSIC  
(b)

**Fig. 2** – C and NC MUSIC spatial spectrum based on MLT(3) for different values of the correlation phase  $\angle\rho$  : (a) and non-circularity phase  $\Delta\phi$  ; (b) of two uncorrelated and highly correlated signal sources with  $|\rho| = \rho' = 0.99$ ,  $\theta_1 = 1.5708\text{rad}$  and  $\theta_2 = \theta_1 + \Delta\theta$  with  $\Delta\theta = 0.3\text{rad}$  when the noise term follows a  $\mathbb{C}t_{M,\nu}$  with  $\nu = 3$  and  $\text{SNR} = 20\text{ dB}$ .

Fig. 3 shows that for two strongly correlated sources, C MUSIC is unable to resolve both sources for a small DOA separation compared to the NC MUSIC algorithm which continues to resolve these sources even for a small DOA separation, e.g.  $\Delta\theta = 0.05$  rad .

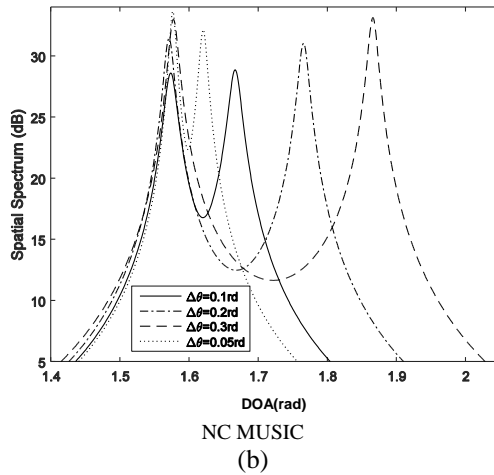
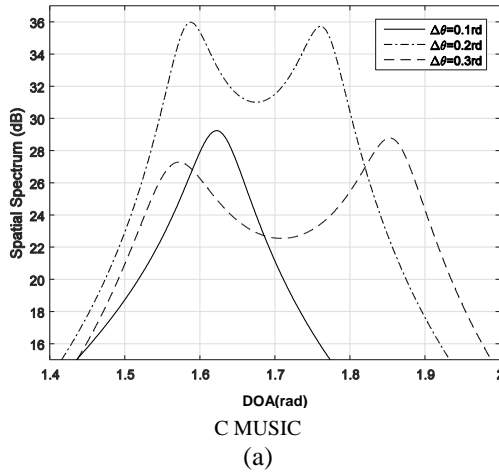


**Fig. 3** – *C* and *NC* MUSIC spatial spectrum based on *MLT(3)* for various values of *DOA* separation  $\Delta\theta$  when the noise term follows a  $\mathcal{C}t_{M,\nu}$  with  $\nu = 3$ . Two sources are highly correlated with  $\angle\rho = \Delta\varphi = \pi/2$ ,  $|\rho| = \rho' = 0.95$  and  $SNR=20$ dB.

Figure 4 shows the impact of the number of sensor arrays *M* on the resolution of *C* MUSIC and *NC* MUSIC algorithms in an environment of strongly correlated sources. It is seen that the resolution ability of these two algorithms strongly

depends on  $M$  and will be the highest with C MUSIC when  $M = 12$  and with NC MUSIC when  $M = 8$ .

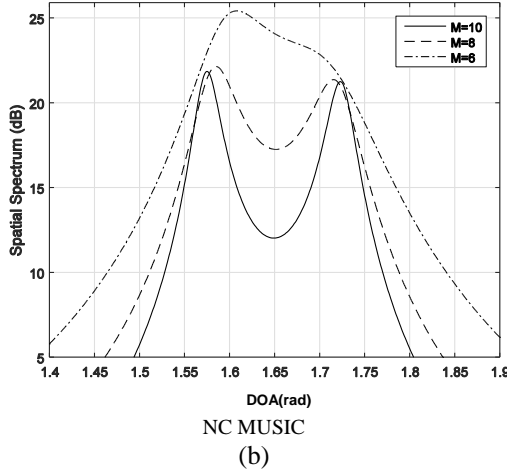
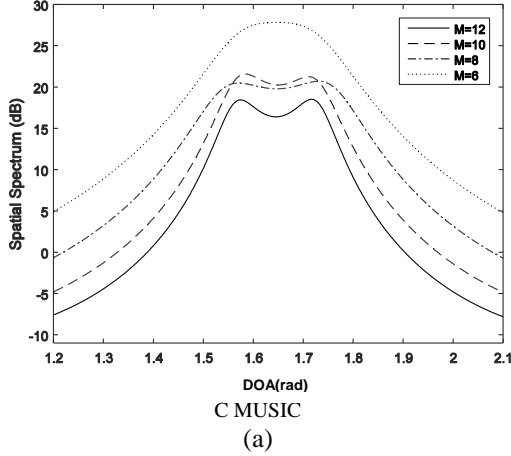


**Fig. 4** – C and NC MUSIC spatial spectrum based on MLT(3) for various values of the number of the sensor array  $M$  when the noise term follows a  $\mathbb{C}t_{M,\nu}$  with  $\nu = 3$ .

Two sources are highly correlated with:  
 $\angle \rho = \Delta \phi = 0$ ,  $|\rho| = \rho' = 0.99$ ,  $\Delta \theta = 0.15$  rad and  $SNR = 20$  dB.

In Fig. 5, the observations  $z_t$  are assumed to follow either a C or a NC  $\mathbb{C}t_{M,\nu}$  with  $\nu = 2.1$ , with associated structured CM  $R_z$  given by (7), or extended CM  $R_{\tilde{z}}$  given by (10), respectively. The estimated projector  $\Pi_T$  [resp.  $\tilde{\Pi}_T$ ] are obtained using the ML M-estimate MLT (2.1) in (4) [resp. (5)]. One can observe

that the C MUSIC algorithm based on Student's ML-estimator is incapable of estimating closed-spaced DOAs (i.e., for small  $\Delta\theta$ ) for uncorrelated and strongly correlated sources, unlike the NC MUSIC algorithm.

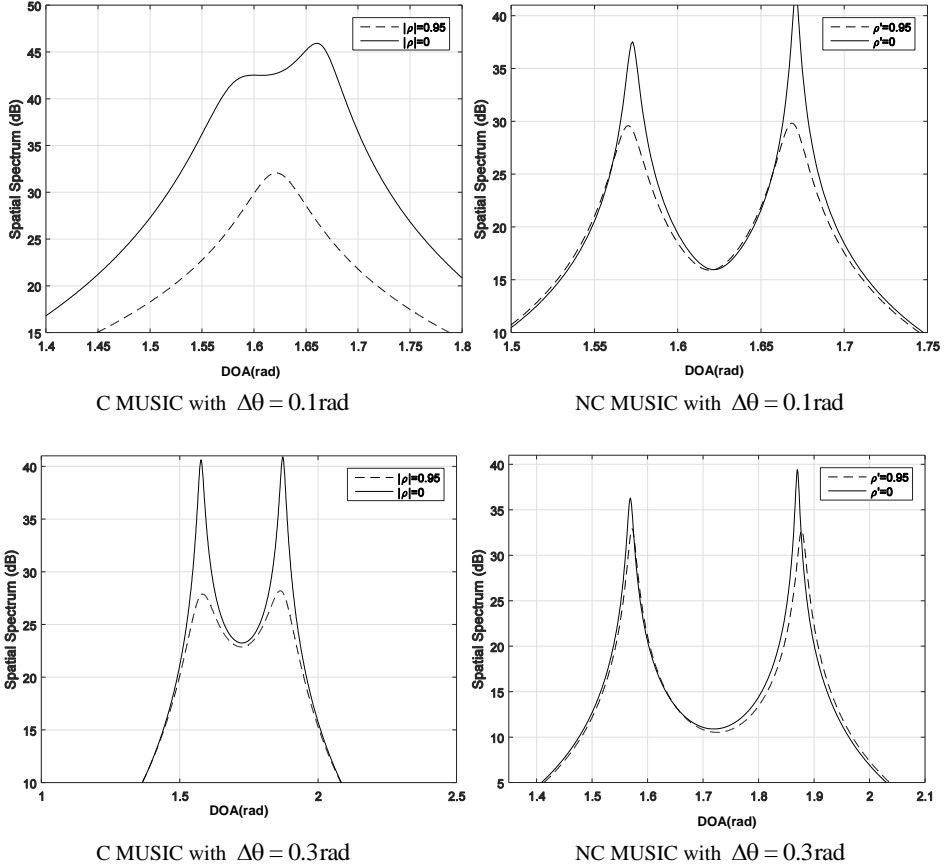


**Fig. 5** – C and [resp., NC] MUSIC spatial spectrum for C  $\mathcal{C}t_{M,\nu}$  [resp., NC  $\mathcal{C}t_{M,\nu}$ ] distributed observations with  $\nu = 2.1$ , using the ML M-estimate MLT(2.1) for two values of the correlation magnitude with:  $\angle\rho = \Delta\varphi = \pi/2$ ,  $\theta_1 = 1.5708\text{rad}$  and  $\theta_2 = \theta_1 + \Delta\theta$ .

## 6 Conclusion

Numerical studies on the dependence of the performance of the C and NC MUSIC-based DOA estimation methods on the correlation magnitude and phase of correlated signal sources are presented. It then quantifies the robustness of these methods in the C CES noise environment, by employing the M – estimators instead of SCM. It is observed that the DOA estimation accuracy degrades

significantly with the C MUSIC algorithm compared with that of the NC MUSIC algorithm when the correlation magnitude increases. It is also noted that the correlation phase affects strongly the DOA accuracy, especially for fewer sensor array elements, and that this effect remains strong with the C MUSIC algorithm that needs a higher number of sensors array elements to estimate the DOA of closely-spaced strongly correlated sources. It is also observed that the NC MUSIC algorithm provides reliable estimates of the DOA's for both far or close correlated sources using the robust ML-estimators, Tyler's and Huber's estimators, and SSCM estimator, which is not the case of the C MUSIC algorithm which fails to produce reliable estimates of DOAs of two strongly correlated closely-spaced sources even with the use of M-estimators.

## **7 References**

- [1] R. Schmidt: Multiple Emitter Location and Signal Parameter Estimation, *IEEE Transactions on Antennas and Propagation*, Vol. 34, No. 3, March 1986, pp. 276–280.
- [2] P. Gounon, C. Adnet, J. Galy: Localization Angulaire de Signaux Non Circulaires, *Traitement du Signal*, Vol. 15, No. 1, 1998, pp. 17–23.
- [3] H. Abeida, J.- P. Delmas: MUSIC-Like Estimation of Direction of Arrival for Noncircular Sources, *IEEE Transactions on Signal Processing*, Vol. 54, No. 7, July 2006, pp. 2678–2690.
- [4] H. Abeida, J.- P. Delmas: Statistical Performance of MUSIC-Like Algorithms in Resolving Noncircular Sources, *IEEE Transactions on Signal Processing*, Vol. 56, No. 9, September 2008, pp. 4317–4329.
- [5] C. A. Balanis, P. I. Ioannides: *Introduction to Smart Antennas*, 1<sup>st</sup> Edition, Morgan & Claypool Publishers, 2007.
- [6] M. Shaghghi, S. A. Vorobyov: Subspace Leakage Analysis and Improved DOA Estimation with Small Sample Size, *IEEE Transactions on Signal Processing*, Vol. 63, No. 12, June 2015, pp. 3251–3265.
- [7] B. Vikas, D. Vakula: Performance Comparison of MUSIC and ESPRIT Algorithms in Presence of Coherent Signals for DoA Estimation, *Proceedings of the International Conference of Electronics, Communication and Aerospace Technology (ICECA)*, Coimbatore, India, April 2007, pp. 403–405.
- [8] J.- J. Fuchs: On the Use of the Global Matched Filter for DOA Estimation in the Presence of Correlated Waveforms, *Proceedings of the 42<sup>nd</sup> Asilomar Conference on Signals, Systems and Computers*, Pacific Grove, USA, October 2008, pp. 269–273.
- [9] X. Chen, J. Xin, N. Zheng, A. Sano: Direction-of-Arrival Estimation of Coherent Narrowband Signals with Arbitrary Linear Array, *Proceedings of the IEEE International Workshop on Signal Processing Systems (SiPS)*, Lorient, France, October 2017, pp. 1–5.
- [10] S. Li, B. Lin: On Spatial Smoothing for Direction-of-Arrival Estimation of Coherent Signals in Impulsive Noise, *Proceedings of the IEEE Advanced Information Technology, Electronic and Automation Control Conference (IAEAC)*, Chongqing, China, December 2015, pp. 339–343.
- [11] M. Rupi, P. Tsakalides, E. Del Re, C. L. Nikias: Robust Spatial Filtering of Coherent Sources for Wireless Communications, *Signal Processing*, Vol. 80, No. 3, March 2000, pp. 381–396.

- [12] T.- J. Shan, T. Kailath: Adaptive Beamforming for Coherent Signals and Interference, *IEEE Transactions on Acoustics, Speech, and Signal Processing*, Vol. 33, No. 3, June 1985, pp. 527–536.
- [13] T.- J. Shan, M. Wax, T. Kailath: On Spatial Smoothing for Direction-of-Arrival Estimation of Coherent Signals, *IEEE Transactions on Acoustics, Speech, and Signal Processing*, Vol. 33, No. 4, August 1985, pp. 806–811.
- [14] J. E. Evans, J. R. Johnson, D. F. Sun: High Resolution Angular Spectrum Estimation Techniques for Terrain Scattering Analysis and Angle of Arrival Estimation, *Proceedings of the 1<sup>st</sup> ASSP Workshop on Spectral Estimation*, Hamilton, Canada, August 1981, pp. 134–139.
- [15] S. U. Pillai, B. H. Kwon: Forward/Backward Spatial Smoothing Techniques for Coherent Signal Identification, *IEEE Transactions on Acoustics, Speech, and Signal Processing*, Vol. 37, No. 1, January 1989, pp. 8–15.
- [16] R. A. Maronna: Robust M-Estimators of Multivariate Location and Scatter, *The Annals of Statistics*, Vol. 4, No. 1, January 1976, pp. 51–67.
- [17] E. Ollila, D. E. Tyler, V. Koivunen, H. V. Poor: Complex Elliptically Symmetric Distributions: Survey, New Results and Applications, *IEEE Transactions on Signal Processing*, Vol. 60, No. 11, November 2012, pp. 5597–5625.
- [18] H. Abeida, J.- P. Delmas: Efficiency of Subspace-Based Estimators for Elliptical Symmetric Distributions, *Signal Processing*, Vol. 174, September 2020, pp. 107644: 1–9.
- [19] H. Abeida, J.- P. Delmas: Slepian-Bangs Formula and Cramer-Rao Bound for Circular and Non-Circular Complex Elliptical Symmetric Distributions, *IEEE Signal Processing Letters*, Vol. 26, No. 10, October 2019, pp. 1561–1565.
- [20] E. Ollila, V. Koivunen: Generalized Complex Elliptical Distributions, *Proceedings of the Sensor Array and Multichannel Signal Processing Workshop*, Barcelona, Spain, July 2004, pp. 460–464.
- [21] P. R. Krishnaiah, J. Lin: Complex Elliptically Symmetric Distributions, *Communications in Statistics - Theory and Methods*, Vol. 15, No. 12, December 1986, pp. 3693–3718.
- [22] A. van den Bos: The Multivariate Complex Normal Distribution - A Generalization, *IEEE Transactions on Information Theory*, Vol. 41, No. 2, March 1995, pp. 537–539.
- [23] E. Ollila, V. Koivunen: Influence Function and Asymptotic Efficiency of Scatter Matrix Based Array Processors: Case MVDR Beamformer, *IEEE Transactions on Signal Processing*, Vol. 57, No. 1, January 2009, pp. 247–259.
- [24] E. Ollila, V. Koivunen: Complex ICA Using Generalized Uncorrelating Transform, *Signal Processing*, Vol. 89, No. 4, April 2009, pp. 365–377.
- [25] H. Abeida, J.- P. Delmas: Robustness of Subspace-Based Algorithms with Respect to the Distribution of the Noise: Application to DOA Estimation, *Signal Processing*, Vol. 164, November 2019, pp. 313–319.
- [26] H. Abeida, J.- P. Delmas: Robustness and Performance Analysis of Subspace-Based DOA Estimation for Rectilinear Correlated Sources in CES Data Model, *Signal Processing*, Vol. 178, January 2021, pp. 107799: 1–12.
- [27] R. A. Horn, C. R. Johnson: *Matrix Analysis*, Cambridge University Press, New York, 1985.
- [28] S. Visuri, H. Oja, V. Koivunen: Subspace-Based Direction-of-Arrival Estimation Using Nonparametric Statistics, *IEEE Transactions on Signal Processing*, Vol. 49, No. 9, September 2001, pp. 2060–2073.